AER Benchmark Specification Sheet

1. Test ID: AER-DYN-002

2. Short Description:

A three-dimensional hexagonal dynamic benchmark describing the ejection of a peripheral control rod in a VVER-440 core with neutron kinetics and simple adiabatic Doppler feedback. The initially critical reactor experiences a power excursion without any reactor scram. The power of the reactor is limited by the continuous accumulation of heat in the fuel.

3. Submitted by: Ulrich Grundmann, FZ Rossendorf, Institute of Safety Research, Germany
Date: 19.10.1999

4. Reviewed by: Pertti Siltanen, Fortum Engineering Ltd Finland
Date: 15.02.2000

5. Accepted by: Mihály Makai, KFKI Atomic Energy Research Institute, Hungary
Date: 15.02.2000

6. Objective:

Comparison of three-dimensional neutron kinetic codes for a rod ejection accident with a simple Doppler feedback mechanism which is the most important feedback mechanism for this type of transients [1]. The assumption of adiabatic fuel temperature heating do not require a detailed thermohydraulic model in the neutron kinetic code.

7. Rationale for Test Setup:

Three-dimensional analysis of transients avoids conservative assumptions required for the application of simpler models. Considering the speed of computation and the size of memories of the available computers three-dimensional analysis of accidents in nuclear reactors can be performed with acceptable computation time. Due to consequences of most transients experiments are not available for code validation. Compared with the pure neutron kinetic problem of the previous benchmark (AER-DYN-001) [2] this benchmark can be considered as a step further to the verification of best estimate codes for transient calculations. The generation of a mathematical reference solution was not possible so far by using fine mesh calculations with the help of finite difference or finite element codes.

8. Input:

a, Reactor Core Geometry and Composition

The initial configuration of the considered VVER-440 reactor is close to the standard configuration with fresh fuel. The position of the lower end of the absorber of the control rod bank K6 is 50 cm from the bottom of core. Fig. 1 shows the distribution of the three fuel types 1, 2 and 3 to the homogeneous assemblies. The absorber material is of type 4. The absorber rods are situated in the hexagons surrounded by thick lines. The control assemblies consist of absorber type 4 in the upper part and fuel of type 2 in the lower part. The position of the ejected rod is in the hexagon filled with lines. The axial position of the absorber rods in the lowest horizontal row of fig. 1 can be seen in fig. 2. Axial and radial reflector is described by given boundary conditions.

The standard mesh for the nodal calculation is one node/assembly and $\Delta z = 25\,\text{cm}$ in axial direction. Solutions performed with a finer mesh are also welcome.

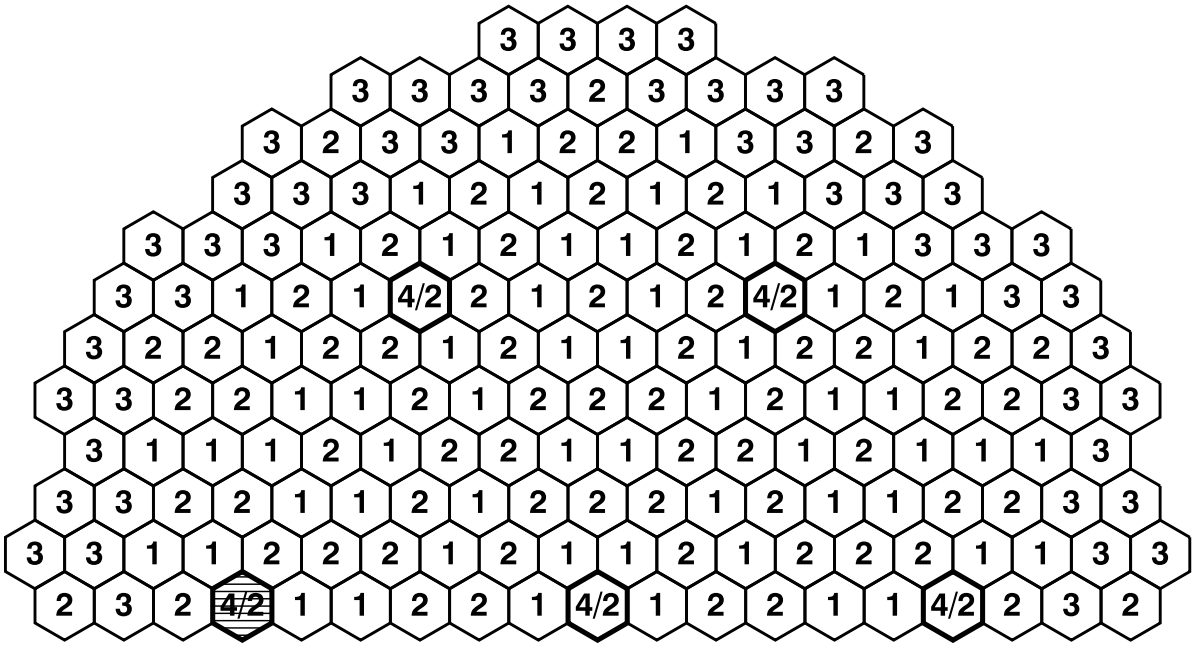

Fig. 1: Core map with the fuel types. Absorbers of bank K6 at positions of types 4/2.

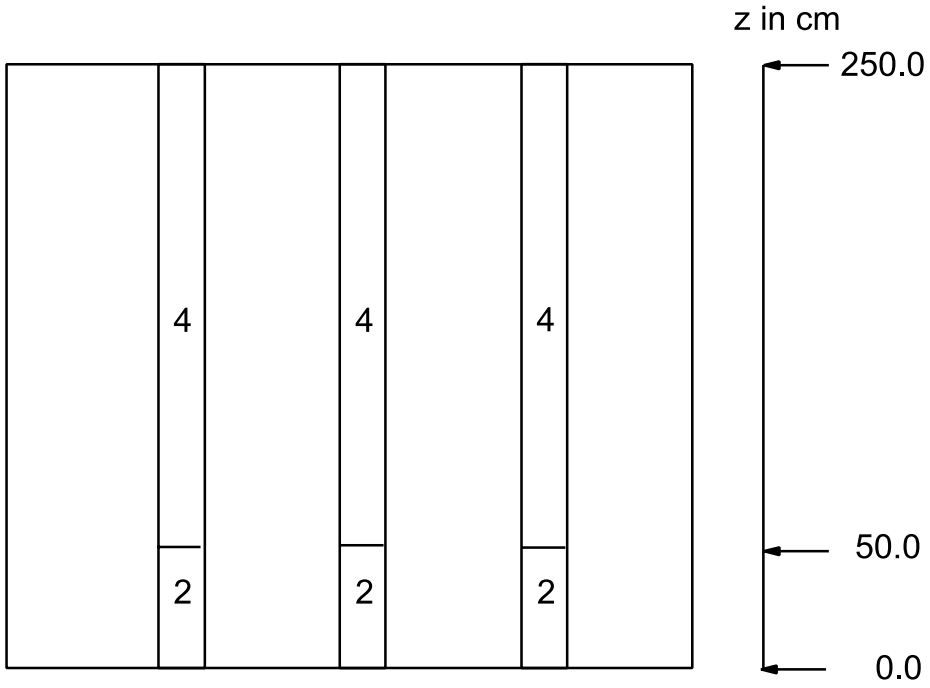

Fig. 2: Axial scheme of core along the lowest row of core map in fig. 1

Table 1: Main fuel parameters

Parameter	Value
Distance between parallel sides of hexagons	14.7 cm
Height of core	250 cm
Number of pins per fuel assembly	126
Outer diameter of fuel pellet	0.76 cm
Inner diameter of fuel pellet	0.14 cm
Density of fuel	10.4 g/cm^3
Heat capacity of fuel	0.3 J/(g ^{o}C)

b, Neutronics Data

The neutron kinetics consists of the solution of the transient neutron diffusion equation for two energy groups which can be described for the benchmark problem in the following form

$$\frac{\partial \varphi_1(\boldsymbol{r},\mathrm{t})}{v_1^n \partial \mathrm{t}} - \nabla D_1^n(\mathrm{t}) \nabla \varphi_1(\boldsymbol{r},\mathrm{t}) + \Sigma_r^n(\mathrm{t}) \varphi_1(\boldsymbol{r},\mathrm{t}) = \frac{1}{\mathrm{k}_{eff}} \sum_{g=1}^{2} \left(1 - ß_g^n\right) \nu\Sigma_{f,g}^n(\mathrm{t}) \varphi_g(\boldsymbol{r},\mathrm{t}) + \sum_{j=1}^{M} \lambda_j c_j(\boldsymbol{r},\mathrm{t})$$

$$\frac{\partial \varphi_2(\boldsymbol{r},\mathrm{t})}{v_2^n \partial \mathrm{t}} - \nabla D_2^n(\mathrm{t}) \nabla \varphi_2(\boldsymbol{r},\mathrm{t}) + \Sigma_a^n(\mathrm{t}) \varphi_2(\boldsymbol{r},\mathrm{t}) = \Sigma_s^n(\mathrm{t}) \varphi_1(\boldsymbol{r},\mathrm{t})$$

$$\frac{\partial c_j(\boldsymbol{r},\mathrm{t})}{\partial \mathrm{t}} = \frac{1}{\mathrm{k}_{eff}} \sum_{g=1}^{2} ß_{g,j}^n \nu\Sigma_{f,g}^n(\mathrm{t}) \varphi_g(\boldsymbol{r},\mathrm{t}) - \lambda_j c_j(\boldsymbol{r},\mathrm{t}) \quad \text{for } j = 1,2,....,\mathrm{M}$$

with

$$ß_g^n = \sum_{\mathrm{j}=1}^{\mathrm{M}} ß_{g,j}^n$$

It is assumed that the cross sections in the nodes n do not depend on space variable. The cross sections and neutron velocities of the 4 types of material are given in table 2. The boundary conditions at the core boundary describing the properties of radial and axial reflectors are contained in table 3. The boundary conditions for treating the absorber rods as inner holes are contained also in this Table. The equivalence with the cross sections of type 4 is based on calculations with the code KIKO3D [2]. The albedo values of a boundary i of a hexagonal node n describe the ratio of the net current and the flux averaged over the side i. The values depend only on the type of boundary, but not on space and time.

$$\alpha_g^i = \frac{\overline{-\mathrm{D}_g^n \nabla \varphi_g(\boldsymbol{r},t)}^{\mathrm{i}}}{\overline{\varphi_g(\boldsymbol{r},t)}^{\mathrm{i}}}$$

The number of delayed neutron groups M = 6. There is only one set of constants for all nodes. The constants of delayed neutrons are given in Table 4. The total yield of delayed neutrons is reduced to ß = 0.005 which increases the reactivity in relation to ß and stands also for the higher content of Plutonium in burnt fuel. The reactivity worth of the absorbers was increased by change of cross sections. It leads to a reactivity insertion of about 2ß by the rod ejection. It was chosen to cover any considered transient of this type in the existing plants.

Table 2: Neutron group constants

	Mat. 1	Mat. 2	Mat. 3	Mat. 4 Absorber
D_1 (cm)	1.3466	1.3377	1.3322	1.1953
D_2 (cm)	0.37169	0.36918	0.36502	0.19313
Σ_r (cm^{-1})	0.025255	0.024709	0.024358	0.222264
Σ_s (cm^{-1})	0.016893	0.015912	0.014888	0.022264
Σ_a (cm^{-1})	0.064277	0.079361	0.10010	0.8
$\nu\Sigma_{f,1}$ (cm^{-1})	0.0044681	0.0055576	0.0070693	0.0
$\nu\Sigma_{f,2}$ (cm^{-1})	0.07407	0.10626	0.15029	0.0
ν_1	2.55	2.55	2.55	
ν_2	2.43	2.43	2.43	
v_1 (cm/s)	1.25E+7	1.25E+7	1.25E+7	1.25E+7
v_2 (cm/s)	2.50E+5	2.50E+5	2.50E+5	2.50E+5

The value of 200 MeV is used for the energy per fission, independently from material type and energy group.

Table 3: Boundary conditions

	Radial Reflector	Axial Reflector	Absorber
α_1	0.18732	0.199840	0.40065
α_2	- 0.081293	- 0.012173	0.30521

Table 4: Constants of delayed neutrons

Group j	1	2	3	4	5	6
$ß_{1,j} = ß_{2,j}$	0.00019	0.001065	0.00094	0.002035	0.00064	0.00013
λ_j (s^{-1})	0.0127	0.0317	0.115	0.311	1.40	3.87

The adiabatic feedback is described by the following dependence for the fission cross section of the second neutron energy group on fuel temperature

$$\Sigma_{f,2}^{n}(t) = \Sigma_{f,2}^{n,0}\left[1+\gamma\left(\sqrt{T_f^n(t)}-\sqrt{T_{f,0}}\right)\right]$$

with $T_{f,0} = 260$ °C and $\gamma = -7.228 \cdot 10^{-4}\ (°\mathrm{C})^{-\frac{1}{2}}$.

$\Sigma_{f,2}^{n,0}$ is the fission cross section of the thermal energy group given by the values in Table 2. It is assumed that the value of the Doppler constant γ and the reference temperature $T_{f,0}$ is independent from the type of fuel.

c, Initial Conditions and Scenario for the Transient

The transient is initiated by the ejection of the eccentric rod of group K6 in 0.16 s at hot zero power (HZP). The constant speed of 12.5 m/s is assumed. The initial reactor power is 1.375 kW. The feedback mechanism is based on the adiabatic increase of fuel temperature from the initial value of 260 °C. No heat is removed from the fuel. If the code has problems to handle the initial power without any heat transport, the code has to be modified by the developer. The transient is simulated up to t = 2 s.

10. Output

a, Expected Results (primary, secondary)

The following results are requested for comparisons of codes

A) Steady State

A1) Eigenvalue k_{eff} of the initial state.
A2) Eigenvalue k_{eff} of the state with the ejected rod.

B) Time functions

B1) reactor power in MW
B2) integral reactor power in MWs
B3) maximum fuel temperature in deg C
B4) nodal power peaking factor [max. nodal power/core average power] (if possible)
B5) reactivity (if possible) in ß

The time tables are given as separate tables consisting of pairs of time and value. At least one space is required between time and value. The pairs have to be separated by one new line. The FORTRAN formats Ew.d or Fw.d (with changing w and d) should be used for the data.

C) Three-dimensional distributions are requested at the following times:

C1) t = 0.0 s
C2) t = 0.16 s (ejection time)
C3) t = t(P_{max}) (time of power maximum)
C4) t = 0.4 s
C5) t = 2.0 s (defined end of transient)

For each time point, the following three distributions are given:

- normalized nodal powers
- nodal fast flux values
- nodal thermal flux values

The spatial distributions are given separately in the following order:

- in a considered layer the nodes are numbered as shown in core map of fig. 1 from left to right beginning with the row at the top and ending with the row at the bottom.

- the values are given layer by layer starting with the lowest axial layer at the bottom of core.

If a mesh different from the standard is used the results have to be converted to the standard mesh. Normalized distributions have to be normalized to the core average value of 1 (nodes with absorber belongs to the core volume!). The recommended format of the numbers is F7.4. At least one space or a new line is required between the numbers.

The preferred file form is ASCII (.txt) which can be used directly for computer input. All output is given in one file. For more details, please refer to one of the given outputs.

11. References

[1] Grundmann, U., Rohde, U.; "Definition of the Second Kinetic Benchmark of AER", Proceedings of the 3rd Symposium of AER, KFKI Atomic Research Institute, Budapest (1993)

[2] Kereszturi, A., Telbisz M.; “A Three-Dimensional Hexagonal benchmark Problem”, Proceedings of the 2nd Symposium of AER, KFKI Atomic Research Institute, Budapest (1992)

[3] M. P. Lizorkin, V. N. Semenov, V. S. Ionov, V. I. Lebedev: "Time Dependent Spatial Neutron Kinetic Algorithm for BIPR8 and its Verification", Proceedings of the 2nd Symposium of AER, KFKI Atomic Research Institute, Budapest (1992)

[4] U. Grundmann, U. Rohde: "DYN3D/M2 - a Code for Calculation of Reactivity Transients in Cores with Hexagonal Geometry", IAEA Technical Committee Meeting on Reactivity Initiated Accidents, Wien 1989Report ZfK - 690, Rossendorf 1989

[5] R. Kyrki-Rajamäki: "VVER Reactor Dynamics Code for Three-Dimensional Transients", Proceedings of the 1st Symposium of AER, KFKI Atomic Research Institute, Budapest (1991).

[6] A. Keresztúri, L. Jakab: "A Nodal Method for Solving the Time-Depending Diffusion Equation in IQS Approximation", Proceedings of the 1st Symposium of AER, KFKI Atomic Research Institute, Budapest (1991)

[7] U. Grundmann, "Results of the Second Kinetic AER-Benchmark", Proceedings of the 4th Symposium of AER, KFKI Atomic Research Institute, Budapest (1994).

12. Recommended Solution

No reference solution is available so far. Therefore the comparison of the results of different nodal codes is considered as an important step of code verification.

13. Summary of Available Solutions

Results of the following codes were obtained and analyzed by comparisons:

- BIPR8 Russian Research Center "Kurchatov Institute", Moscow, (Russia)
  Code BIPR8 /3/
- DYN3D/M2 Forschungszentrum Rossendorf, Institute of Safety Research,
  Rossendorf (Germany)
  Code DYN3D/M2 /4/
- HEXTRAN VVT Energy/ Nuclear Energy, Espoo, (Finland)
  Code HEXTRAN /5/
- KIKO3D KFKI Atomic Energy Research Institute, Budapest, (Hungary)
  Code KIKO3D /6/

Absorber and reflector can be described by cross section data or albedos. The four codes describe the absorbers by using albedos of table 3 or equivalent diffusion constants of table 2. KIKO3D is able to use both of them. Using cross sections in KIKO3D albedos were calculated giving nearly the same eigenvalue in the initial state and the same reactivity effect for the ejected rod. HEXTRAN has used these albedos while DYN3D and BIPR8 have applied cross sections for the absorbers.

Table 5 shows the list of results which were provided for the comparisons. Some of comparisons shown in the following were presented in /7/.

Table 5: List of results

result	BIPR8[*)]	DYN3D	HEXTRAN	KIKO3D
A1	X	X	X	X
A2	X	X	X	X
B1	X	X	X	X
B2	X	X	X	X
B3	X	X	X	X
B4	X[**)]	X	X[**)]	X[**)]
B5		X		X
C1	X	X	X	X
C2	X	X	X	X
C3	X	X	X	X
C4	X	X	X	X
C5	X	X	X	X

[*)] The time history of the inverse period (result B6) and the distributions of power and fluxes at t = 5.0 s (results C6) are given as additional results

[**)] The power peak factors are given at time points t = 0.0 s, 0.16 s, 0.25 s, 0.4 s and 2.0 s (see table 7).

a, integral parameters and time functions

The uncertainties of the obtained results have not been evaluated, since no reference benchmark solution exists. On the basis of selected calculations an intercomparison of different codes , in which the deviations are referred to the results of DYN3D, is presented here.

The intial eigenvalue $k_{eff,0}$ and the eigenvalue of the steady state with the ejected rod are given in table 6. The results of KIKO3D calculated with both albedoes and diffusion constants for absorbers are the same in terms of eigenvalues and reactivities. The static reactivity values and the deviations from DYN3D are given in the right columns. DYN3D and KIKO3D give approximately the same reactivity. The largest difference was obtained by BIPR8, but reactivities of BIPR8 and HEXTRAN differ in the same order as DYN3D and KIKO3D.

Table 6: Static eigenvalue in the initial state ($k_{eff,0}$), in the state with ejected rod ($k_{eff,1}$) and static reactivity worth of the ejected rod ($\Delta\rho$).

Code	$k_{eff,0}$	$k_{eff,1}$	Rod worth $\Delta\rho$ (%) $\Delta\rho = (1 - \frac{k_{eff,0}}{k_{eff,1}})$	$(\frac{\Delta\rho_{Code}}{\Delta\rho_{DYN3D}} - 1) \cdot 100\%$
BIPR8	0.998442	1.008673	1.0143	4.
DYN3D	0.999941	1.009792	0.9755	-
HEXTRAN	0.99902	1.009181	1.0069	3.2
KIKO3D[1]	0.999994	1.009926	0.9834	0.8
KIKO3D[2]	1.000001	1.009933	0.9834	0.8

KIKO3D[1]: Absorbers were taken into account by cross sections
KIKO3D[2]. Equivalent albedos were used for description of absorbers.

A higher reactivity value results in a higher power peak, which can be seen in fig. 3. The higher reactivity gives an earlier peak also. The power peaks of KIKO3D and DYN3D have nearly the same maximum value. The peak of KIKO3D is about 0.01 s earlier, caused possibly by the 0.8 % higher reactivity or the different time integration technique. The highest power peak is given in the result of HEXTRAN, but it is close to the result of BIPR8. Fig. 3 shows that BIPR8 and HEXTRAN on the one side and DYN3D and KIKO3D on the other side should give different values of integral power which can be seen in fig. 4. The differences in integral power are caused mainly by the different peaks. This can be seen also in the curve of maximum fuel temperature versus time (fig. 5). Besides the specific energy release in the fuel, the maximum fuel temperature is an important safety parameter for reactivity initiated accidents. The position of the maximum fuel temperature after rod ejection is the 5th axial layer from the bottom of core in the fuel element which is situated in the lowest row of fig. 1 at the second position from the left hand side. This position was obtained by the results of DYN3D. Considering the power distribution calculated by the other codes the maximum seems to be at the same position.

The 3.2 - 4 % higher reactivity value of HEXTRAN and BIPR8 in comparison to KIKO3D and DYN3D gives a maximum fuel temperature which is about 150 degrees higher.

Considering the differences of maximum fuel temperature the contribution of the global power peak and the influence of the power peaking factor should be investigated. Fig. 6 shows the time behaviour of power peaking factor given by the DYN3D calculation. The maximum value of peaking factor occurs after ejection of the rod. The Doppler feedback, being maximal in the local power peak, reduces the power in the peak more than in other parts of the reactor. The power peaking factor for the other codes were calculated from the spatial distributions given at several time points (table 7). It can be seen that the results of all codes are close to each other except at the time of power maximum. The changes of power peaking factor at power maximum are very fast. Therefore the differences do not influence the other results. Later the deviations of peaking factors are lower than 0.5 %.

b, spatial distributions

Fig. 7 shows the assembly powers of DYN3D and the deviations of the other codes at the initial state. Besides the assemblies with inserted absorbers (hexagons with thick boundary) we see that the differences between DYN3D and KIKO3D are lower than 1.3%. The deviations of the other codes are larger. BIPR8 gives deviations of 6.2% and HEXTRAN -4.5%. The maximum deviations between BIPR8 and HEXTRAN are 1.8%. Analyzing the agreement of results we see that DYN3D and KIKO3D form one group of codes and BIPR8 and HEXTRAN the other. That was suggested also by the results shown in the previous chapter. Nevertheless, the deviations between BIPR8 and HEXTRAN seems to be sometwhat larger than between DYN3D and KIKO3D. The maximal deviations of the assembly powers between both code groups are observed at the boundary and central core regions, but with the opposite sign. The assembly power distribution of DYN3D and the deviations of the other results are shown at ejection time t = 0.16 s (fig. 8), at time of maximum power (fig. 9) and at t = 2.0 s (fig. 10).

Considering the power distribution at the ejection time t = 0.16 s in fig. 8 the higher flux values in the assembly No. 4 (position of ejected rod) of the the codes BIPR8, HEXTRAN in comparison to DYN3D and KIKO3D are leading to larger values of reactivity.

Fig. 11 shows the radial averaged axial powers of DYN3D at the initial state and the deviations of the other codes. We see a good agreement of all results. BIPR8 gives a small deviation in the second layer which is the next layer under the lower end of control rods. The values of averaged power calculated by DYN3D and the relative deviations of the other codes can be seen in table 8. The powers in the first and last layer are small and the relative deviations are also larger between DYN3D and KIKO3D. Considering these distributions at the ejection time t = 0.16 s (table 9), at the time of the maximum power (table 10) and after

power peak at t = 2.0 s (table 11, fig. 12) the deviation at upper and lower layer are similar. Considering the layer under the lower end of control rods, the deviation of BIPR8 is reduced from 1.9 % at t = 0.0 s to 1.3 % at t = 2.0 s, because we have a radial power peak at the position of the ejected rod. If the deviation is influenced by the end of absorbers, it should be reduced, because there is no any absorber in the region of power peak which gives a essential contribution to the radial averaged value.

Table 7: Power peaking factors at different time points.

Time (s)	0.0	0.16	Power maximum (~ 0.25 s)	0.4	2.0
BIPR	2.30	7.76	6.13	5.65	5.29
DYN3D	2.33	7.69	6.53	5.67	5.30
HEXTRAN	2.33	7.77	6.52	5.66	5.32
KIKO3D	2.34	7.78	6.41	5.68	5.30

Table 8: Normalised axial (radially averaged) power distribution of DYN3D and the relative deviations of the other codes for t = 0.0 s.

LAYER	DYN3D	KIKO3D - DYN3D (%)	HEXTRAN - DYN3D (%)	BIPR8 - DYN3D (%)
10	0.299	-1.8	-2.5	-2.5
9	0.645	-0.1	-0.3	-0.5
8	0.948	0.3	0.2	-0.6
7	1.186	0.5	0.3	-0.5
6	1.342	0.5	0.4	-0.4
5	1.405	0.4	0.3	-0.2
4	1.372	0.3	0.1	0.1
3	1.246	-0.1	-0.2	0.7
2	1.021	-0.7	-0.4	1.9
1	0.535	-1.7	-0.1	0.1

Table 9: Normalised axial (radially averaged) power distribution of DYN3D and the relative deviations of the other codes for ejection time t = 0.16 s.

LAYER	DYN3D	KIKO3D - DYN3D (%)	HEXTRAN - DYN3D (%)	BIPR8 - DYN3D (%)
10	0.326	0.3	-1.5	-0.8
9	0.702	1.3	0.2	0.8
8	1.028	1.1	0.4	0.4
7	1.271	0.8	0.4	-0.1
6	1.412	0.4	0.3	0.0
5	1.439	0.1	0.1	-0.1
4	1.352	-0.3	-0.1	-0.2
3	1.160	-0.8	-0.3	-0.1
2	0.875	-1.5	-0.6	0.4
1	0.435	-2.6	-0.5	-1.4

Table 10: Normalised axial (radially averaged) power distribution of DYN3D and the relative deviations of the other codes at maximum power.

LAYER	DYN3D	KIKO3D - DYN3D (%)	HEXTRAN - DYN3D (%)	BIPR8 - DYN3D (%)
10	0.339	-1.2	-2.6	-1.2
9	0.718	0.0	-0.5	0.4
8	1.032	0.2	-0.1	-0.2
7	1.257	0.1	0.1	-0.6
6	1.385	0.1	0.2	-0.8
5	1.411	0.1	0.2	-0.6
4	1.336	0.1	0.2	0.2
3	1.165	0.1	0.1	0.7
2	0.900	-0.1	0.1	2.3
1	0.456	-0.9	0.3	1.1

Table 11: Normalised axial (radially averaged) power distribution of DYN3D and the relative deviations of the other codes for ejection time t = 2.0 s.

LAYER	DYN3D	KIKO3D - DYN3D (%)	HEXTRAN - DYN3D (%)	BIPR8 - DYN3D (%)
10	0.346	-1.1	-2.6	-1.7
9	0.723	0.2	-0.4	0.2
8	1.026	0.3	0.0	-0.1
7	1.238	0.3	0.2	-0.2
6	1.359	0.2	0.2	0.2
5	1.388	0.2	0.2	-0.2
4	1.328	0.1	0.2	-0.0
3	1.179	-0.1	0.1	0.3
2	0.932	-0.4	0.0	1.3
1	0.481	-1.4	0.2	-0.5

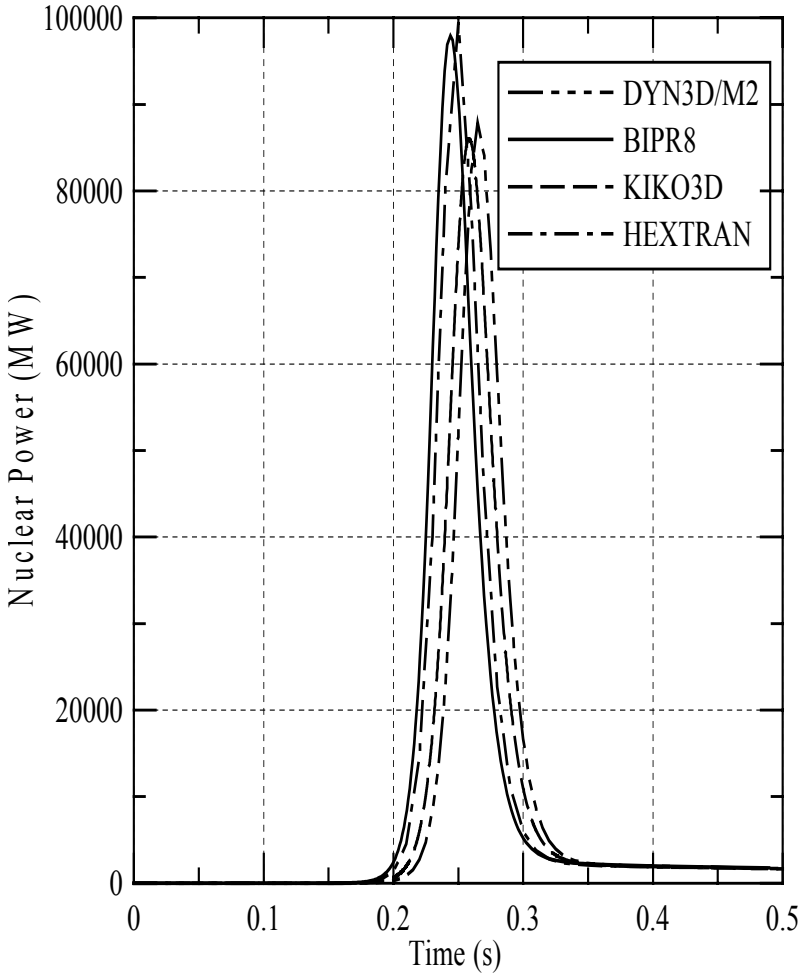

Fig. 3: Nuclear power versus time

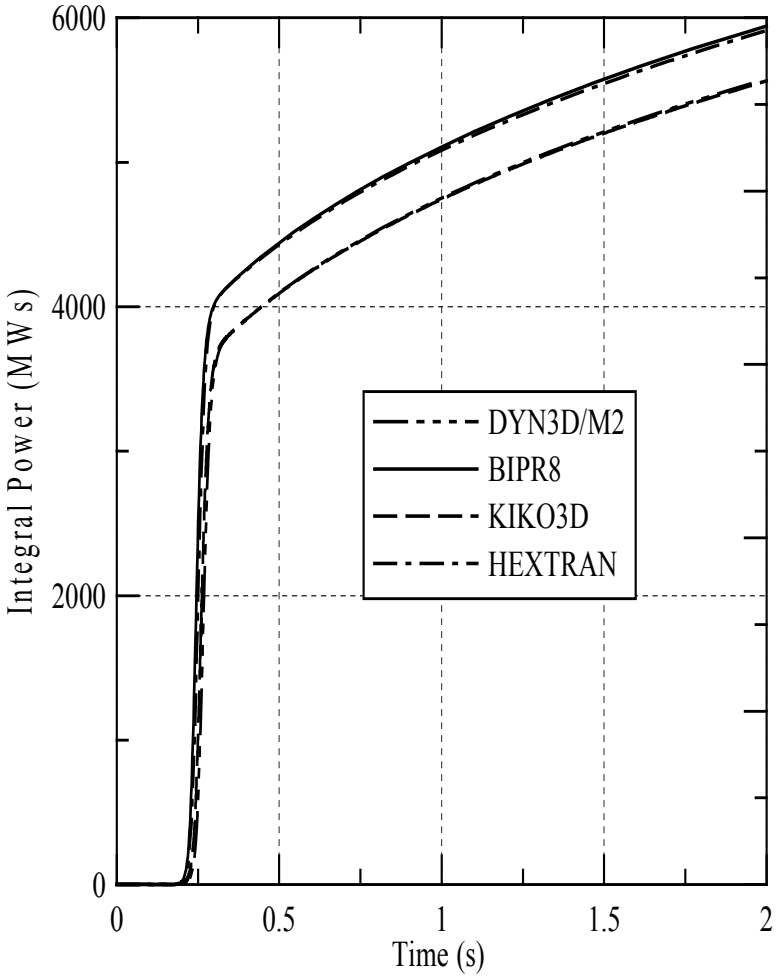

Fig. 4: Integral power versus time

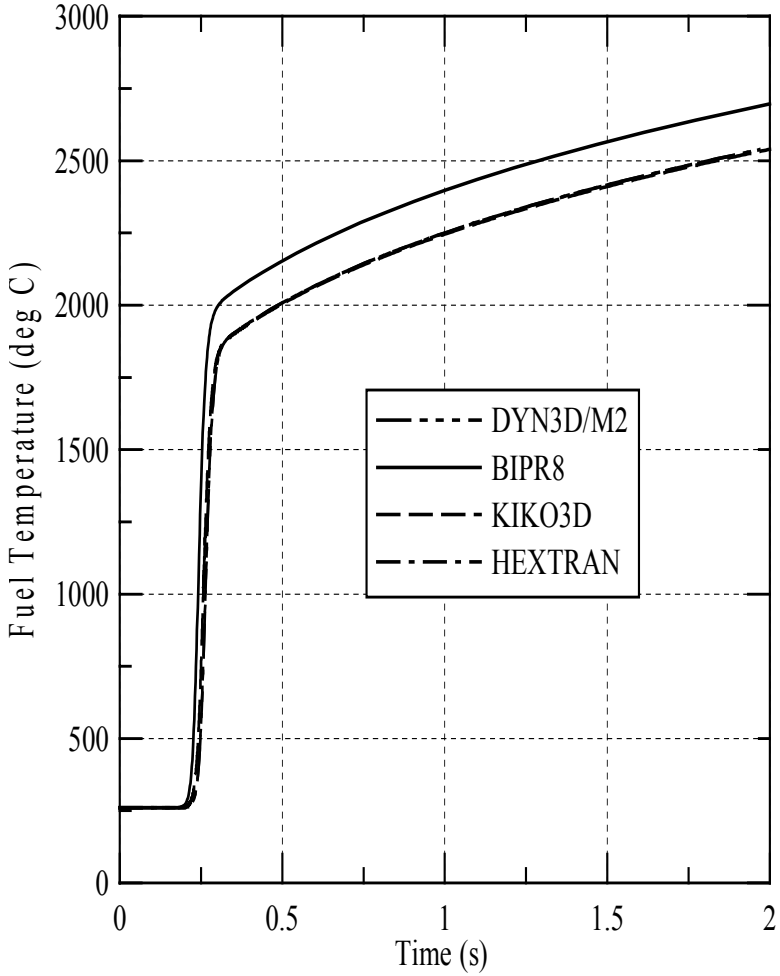

Fig. 5: Maximum fuel temperature versus time

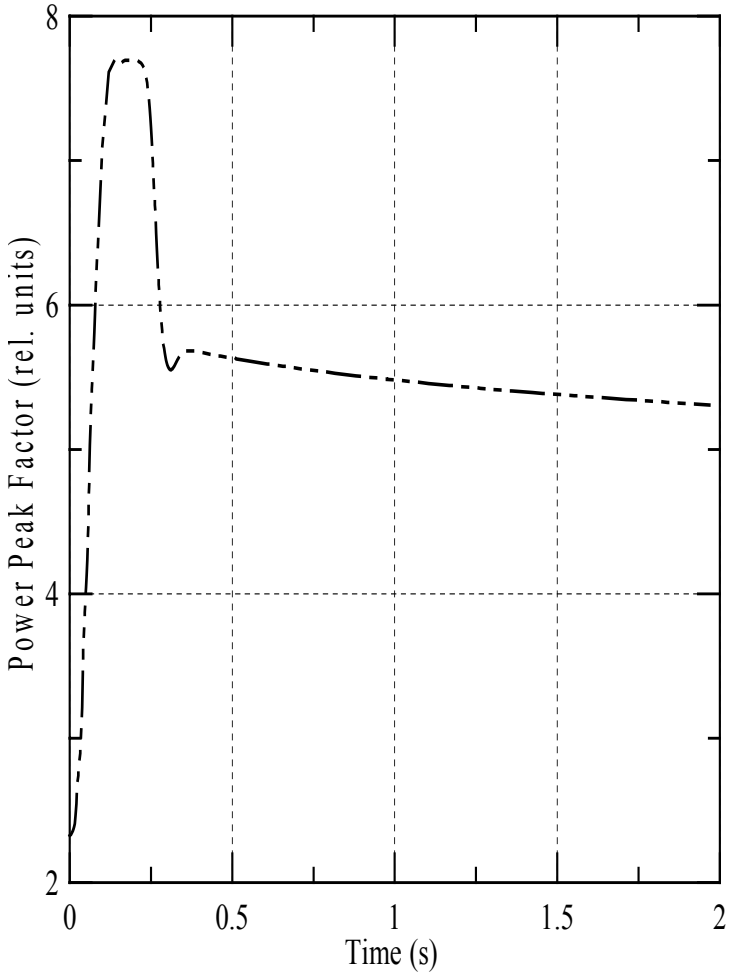

Fig.6: DYN3D/M2 Power peaking factor versus time

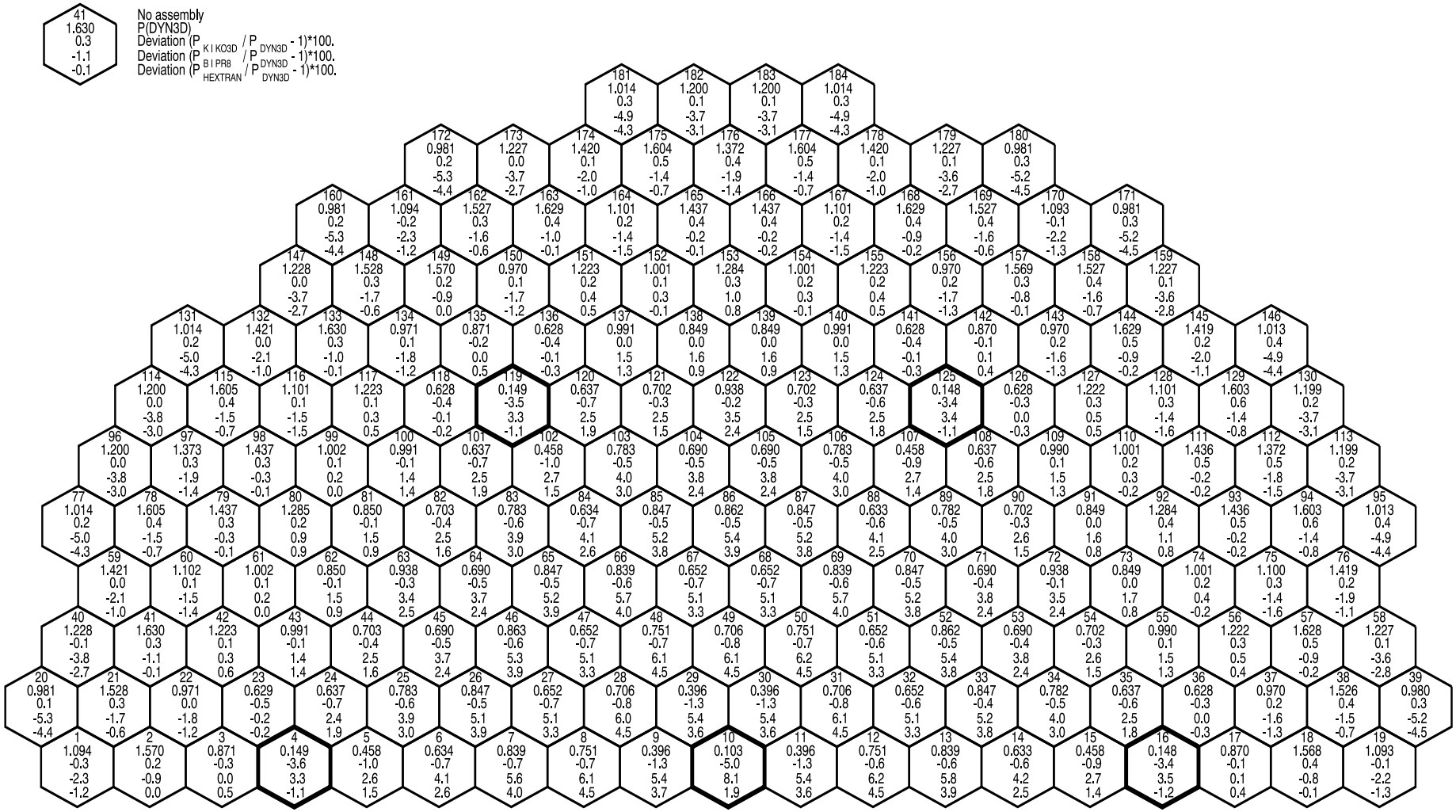

Fig. 7 : Assembly powers of DYN3D with the deviations of the results of the other codes at time t = 0.0 s.

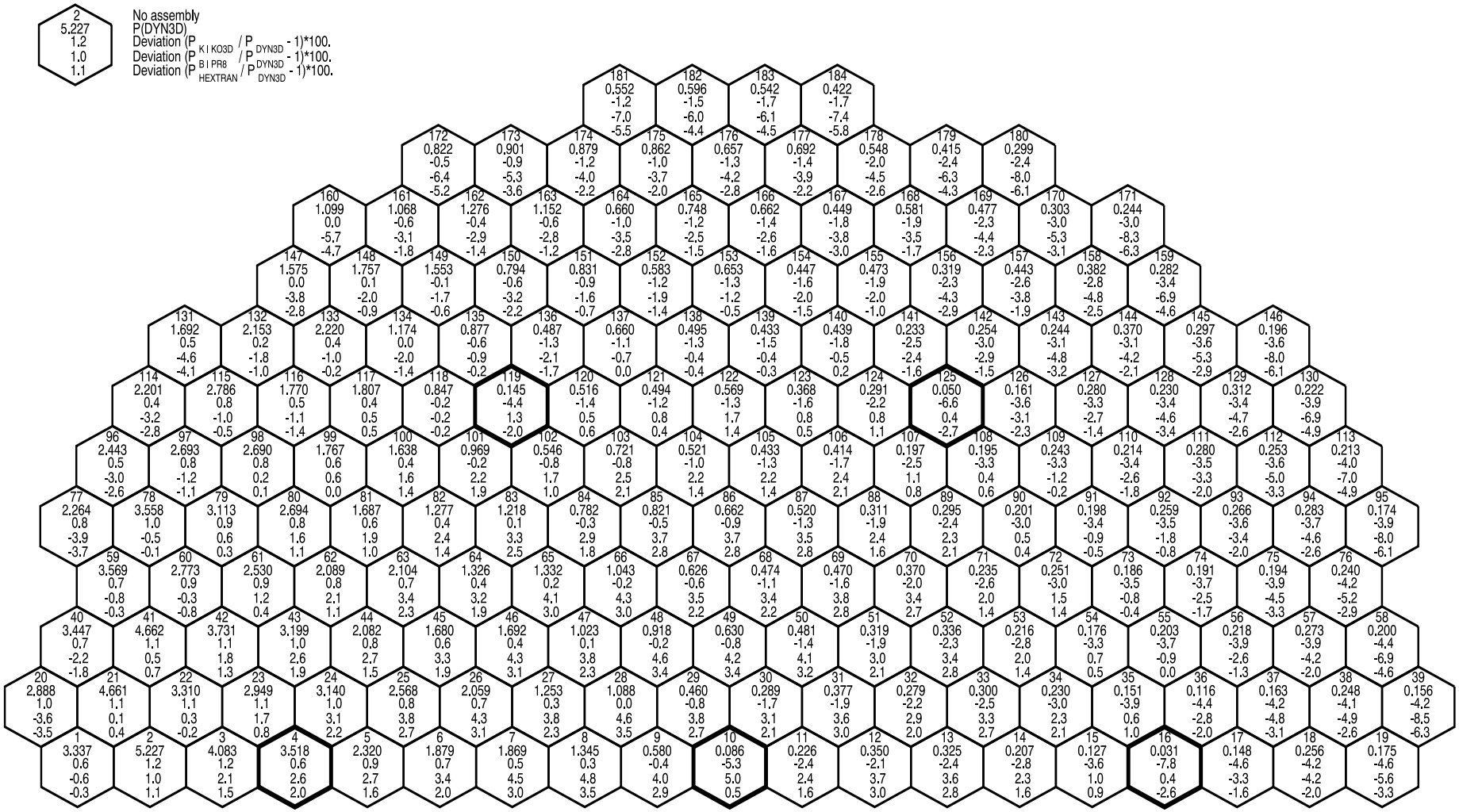

Fig. 8 : Assembly powers of DYN3D with the deviations of the results of the other codes at time t = 0.16 s.

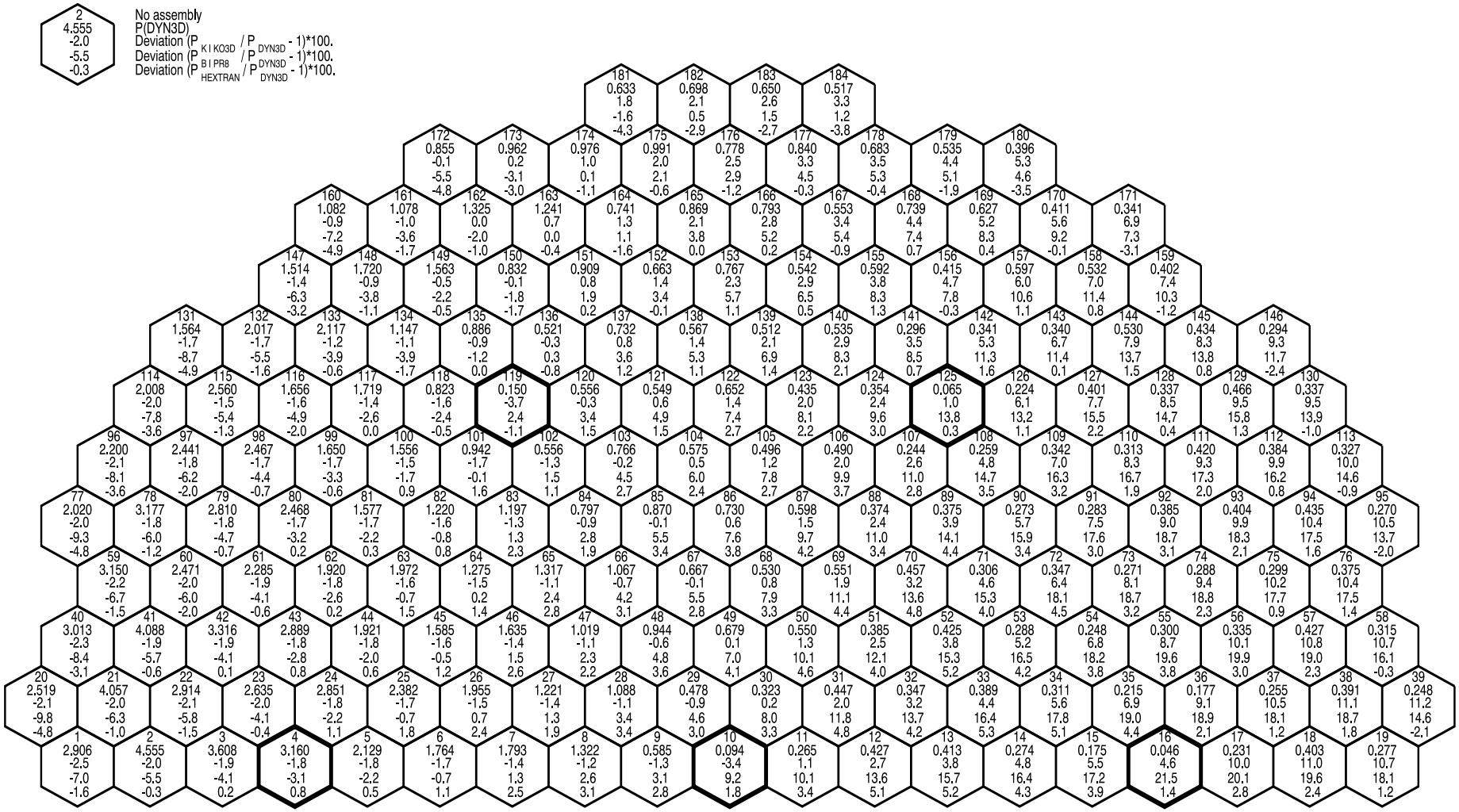

Fig. 9 : Assembly powers of DYN3D with the deviations of the results of the other codes at time of maximum power.

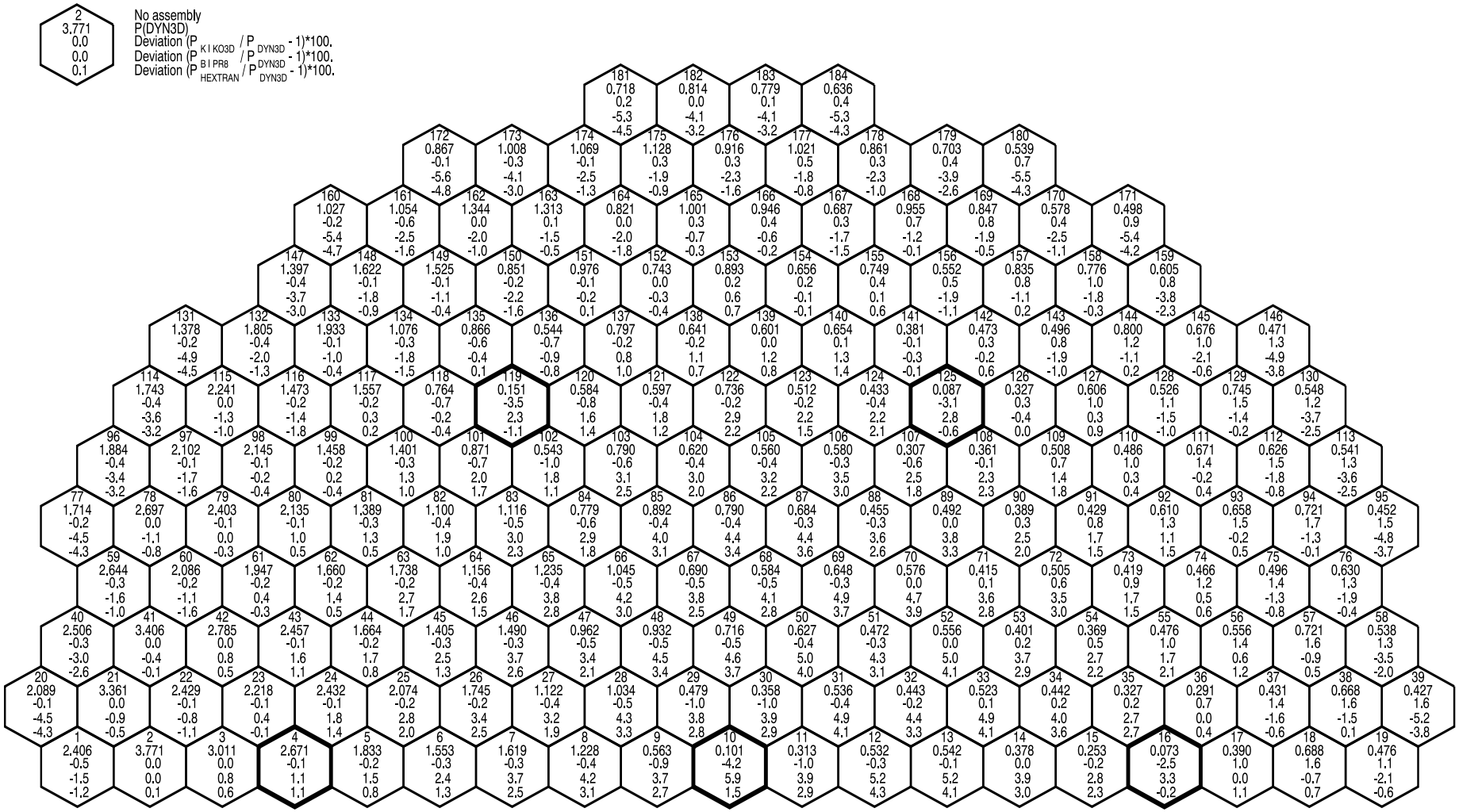

Fig. 10: Assembly powers of DYN3D with the deviations of the results of the other codes at time t = 2.0 s.

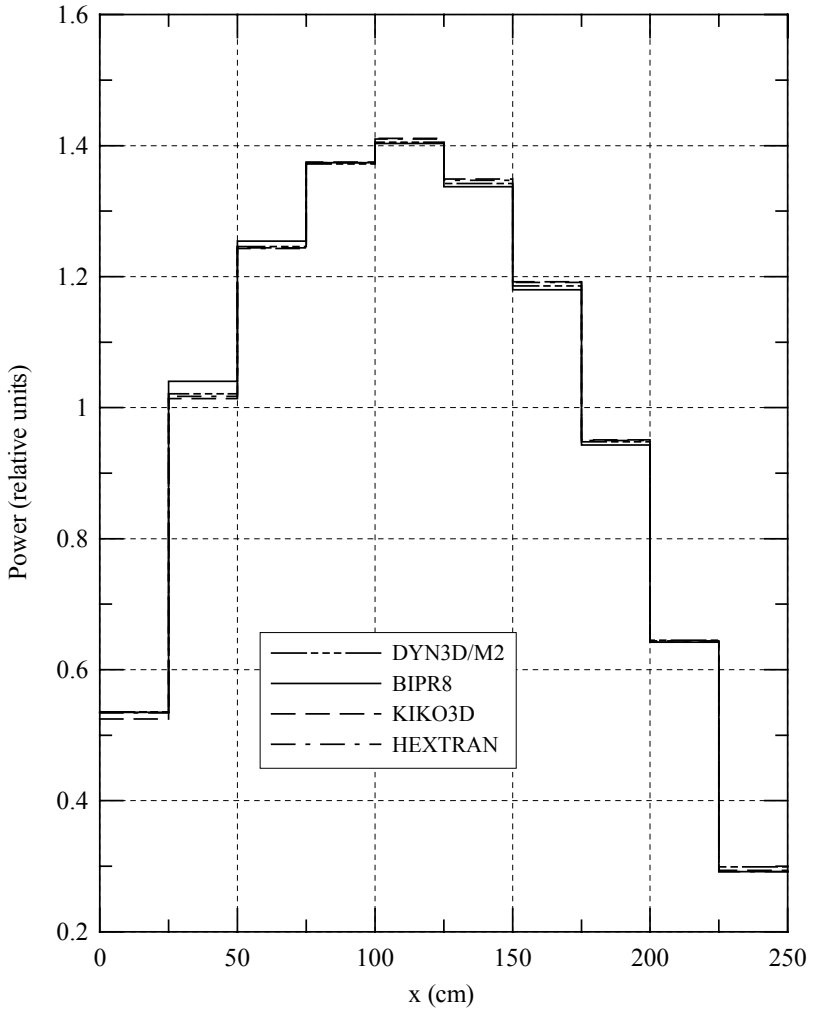

Fig. 11: Normalized axial (radially averaged) power distribution at t = 0.0 s.

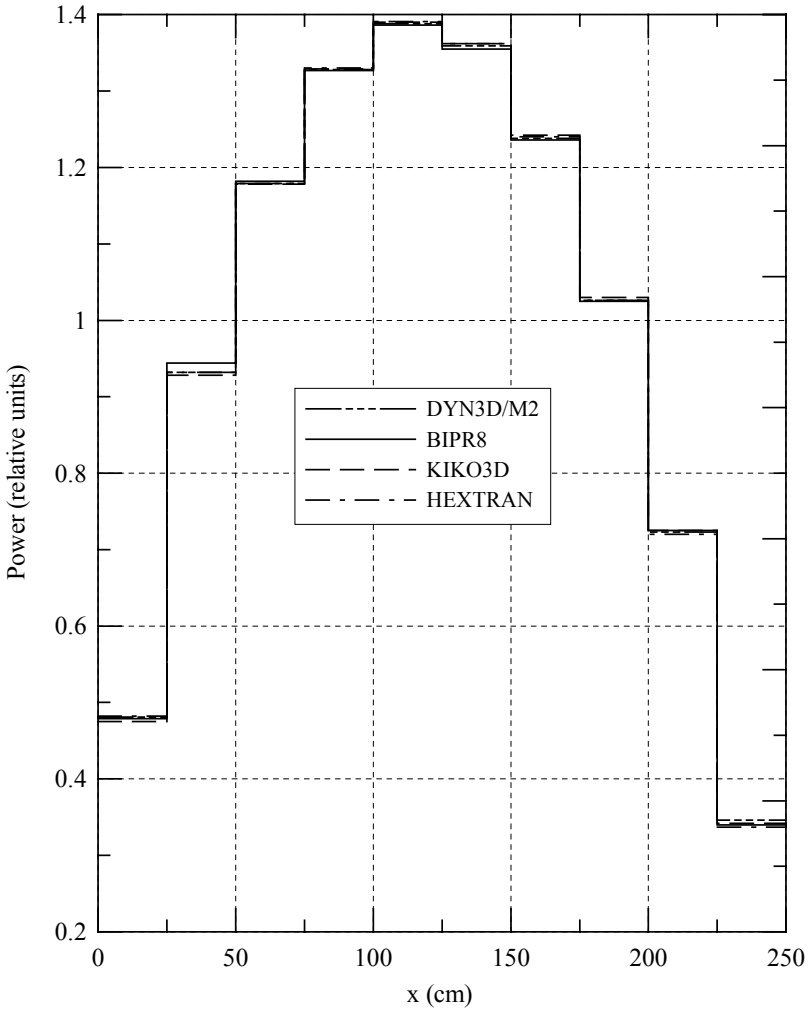

Fig. 12: Normalized axial (radially averaged) power distribution at t = 2.0 s.